Dysfunction of a Peripheral Lipid Sensor Gpr120 Causes Pgd2-microglia-provoked Neuroinflammation

Kensuke Iwasa
Saitama Medical University: Saitama Ika Daigaku
Shinji Yamamoto
Saitama Medical University: Saitama Ika Daigaku
Kota Yamashina
Saitama Medical University: Saitama Ika Daigaku
Chiaki Sakemoto
Saitama Medical University: Saitama Ika Daigaku
Nan Yagishita-kyo
Saitama Medical University: Saitama Ika Daigaku
Kei Maruyama
Saitama Medical University: Saitama Ika Daigaku
Takeo Awaji
Saitama Medical University: Saitama Ika Daigaku
Yoshinori Takei
Toho University: Toho Daigaku
Akira Hirasawa
Kyoto University: Kyoto Daigaku
Keisuke Yoshikawa (keisukey@saitama-med.ac.jp)
Saitama Medical University https://orcid.org/0000-0002-6348-6138

Research article

Keywords: Prostaglandin, G-protein-coupled receptor 120 (GPR120), Neuroinflammation

Posted Date: December 1st, 2020

DOI: https://doi.org/10.21203/rs.3.rs-114598/v1

Abstract

Background

Neuroinflammation is a key pathological component of neurodegenerative disease and is characterized by microglial activation and the secretion of proinflammatory mediators. We previously reported that a surge in prostaglandin D_2 (PGD_2) production and PGD_2-induced microglial activation could provoke neuroinflammation. We also reported that a lipid sensor GPR120 (free fatty acid receptor 4), which is expressed in enteroendocrine cells in the intestine, could be activated by polyunsaturated fatty acids (PUFA), thereby mediating secretion of glucagon-like peptide-1 (GLP-1). Dysfunction of GPR120 results in obesity in both mice and humans. To reveal the relationship between PGD_2-microglia-provoked neuroinflammation and intestinal PUFA/GPR120 signaling, we investigated neuroinflammation and neuronal function in GPR120 knockout (KO) mice.

Results

In the current study, we discovered notable PGD_2-microglia-provoked neuroinflammation (increased PGD_2 production and microglial activation) and neurodegeneration (declines in neurogenesis, hippocampal volume, and cognitive function) in GPR120 KO mice. We also found that Hematopoietic-prostaglandin D synthase (H-PGDS) was expressed in microglia, microglia were activated by PGD_2, H-PGDS expression was upregulated in GPR120 KO hippocampus, and inhibition of PGD_2 production attenuated this neuroinflammatory pathway, suggesting that PGD_2-microglia-provoked neuroinflammation was constantly occurring in the hippocampus of GPR120 KO mice. GPR120 mRNA was detected in the intestinal tissues, but not in the brain tissue of WT mice. GPR120 KO mice exhibited reduced intestinal, plasma, and intracerebral GLP-1 levels. Peripheral administration of a GLP-1 analogue, liraglutide, reduced PGD_2-microglia-provoked neuroinflammation and further neurodegeneration in GPR120 KO mice.

Conclusions

Our results suggest that PGD_2-microglia-provoked neuroinflammation and neurodegeneration observed in GPR120 KO mice are probably caused by defects in intestinal GPR120 function, and not in the CNS. Our results also suggest that GLP-1 secretion, stimulated by intestinal GPR120, may remotely contribute to suppression of PGD_2-microglia-provoked neuroinflammation and further neurodegeneration in the hippocampus.

Background

Prostaglandins (PGs) are arachidonic acid (AA)-derived lipid mediators that exert diverse biological activities through their cognate G-protein-coupled receptors (GPCRs) [1]. PGD_2, one of the most abundant PGs in the brain, is generated by two PGD synthesis (PGDSs), hematopoietic- and lipocalin-type PGDS (H-PGDS and L-PGDS, respectively), and signals through two distinct GPCRs, DP1 and DP2 (CRTH2) [2, 3].

Neuroinflammation, as typified by microglial activation and secretion of proinflammatory mediators, is a major contributor to neurodegeneration [4]. Neurodegeneration refers to the loss of neuronal function caused by atrophy (reduced brain volume), neuronal death, or impaired neurogenesis, which are hallmarks of neurodegenerative disease [4, 5, 6]. Activated microglia secrete proinflammatory mediators, such as PGs, and mediate neuronal injury, which exacerbates neurodegeneration [7]. We previously reported that a surge in PGD_2 production and PGD_2-induced microglial activation provoke neuroinflammation and further neurodegeneration in excitotoxic hippocampal lesion [8, 9, 10]. Thus, a surge in PGD_2 production and microglial activation are closely connected with neuroinflammation and neurodegeneration.

We also previously reported that GPR120 (free fatty acid receptor 4) is expressed in intestinal enteroendocrine cells [11] and is a receptor of polyunsaturated fatty acids (PUFA), such as α-linolenic acid, eicosapentaenoic acid (EPA), docosahexaenoic acid (DHA), and AA [11, 12]. GPR120 senses PUFA and mediates the secretion of an incretin, glucagon-like peptide-1 (GLP-1), which promotes insulin secretion [11, 13]. Furthermore, dysfunction of GPR120 results in dietary obesity in both mice and humans [13]. Recently, GLP-1 biological activity has become the basis for incretin-based therapies for type 2 diabetes mellitus, including liraglutide, an agonist of the GLP-1 receptor [14, 15]. In addition to peripheral GLP-1 levels, GLP-1 readily crosses the blood-brain barrier (BBB) and stimulates the GLP-1 receptor expressed in the brain [16, 17]. Potentiation of intracerebral GLP-1 bioactivity has been shown to increase neuronal activity, promote neuronal growth, and have neuroprotective properties [18, 19].

In the current study, we evaluated neuroinflammation and neuronal function in GPR120 KO mice to reveal the relationship between PGD_2-microglia-provoked neuroinflammation and intestinal PUFA/GPR120 signaling.

Methods

Animal procedures

Mice lacking GPR120 are described previously [13]. The established mixed C57BL/6/129 background GPR120 KO mice were backcrossed into the C57BL/6J background using a marker-assisted breeding approach [20]. Genotyping of the GPR120 KO mice was performed using the primers, Forward: 5'-aagtcaatcgcacccacttc-3' Reverse: 5'-caagctcagcgtaagcctct-3'. We confirmed that GPR120 gene was knockout in GPR120 KO mice (Additional file 1: Fig. S1A). Male WT C57BL/6J (Tokyo Laboratory Animals Science, Tokyo, Japan) and GPR120 KO mice were maintained on a 12 h/12 h light/dark cycle with free access to a powdered diet (CLEA Japan, Tokyo, Japan) and tap water. 16-weeks old male WT and GPR120 KO mice were used for all experiments.

Pharmacological treatments

5-weeks old mice were placed on a powdered diet containing 0.01% indomethacin (Nacalai tesque, Tokyo, Japan) for a total period of 11 weeks for indomethacin treatment studies. For liraglutide studies, 5-weeks

old mice were inserted subcutaneously an Alzet osmotic pump (Muromachi, Tokyo, Japan) filled saline dissolved liraglutide (Novo Nordisk, Bagsværd, Danmark) in the abdomen. The pumps delivered saline or 200 mg/kg of liraglutide per day for 11 weeks. Sitagliptin phosphate monohydrate (SPM, 50 mg/kg per day, ApexBio, Boston, MA, USA) was orally administrated to 15-weeks old mice for a week. The dose of liraglutide and SPM was based on previous reports [21, 22].

Antibodies

We used the following antibodies: anti-Ionized calcium binding adapter molecule 1 (Iba-1, 019-19741, Wako, Osaka, Japan), anti-Glial fibrillary acidic protein (GFAP, ab68428, Abcam, Cambridge, MA), anti-cyclooxygenase-1 (COX-1, sc-19998, Santa Cruz Biotechnology, CA), anti-COX-2 (sc-376861, Santa Cruz Biotechnology, CA), anti-L-PGDS (PA1-46023, Thermo Fisher Scientific, Tokyo, Japan), anti-H-PGDS (PA5-24347, Thermo Fisher Scientific, Tokyo, Japan), anti-doublecortin (DCX, ab18723, Abcam, Cambridge, MA), anti-Ki67 (NB500-170, Novus Biologicals, Inc., Littleton, CO), anti-superoxide dismutase 2 (SOD2, 13194, Cell Signaling Technology, Beverly, MA), anti-14-3-3ζ (7413, Cell Signaling Technology, Beverly, MA), anti-synaptophysin (ab32127, Abcam, Cambridge, MA), anti-postsynaptic density protein 95 (PSD95, 610495, BD Biosciences, San Diego, CA), anti-α-tubulin (T5168, Sigma-Aldrich, Deisen-hofen, Germany), and anti-GAPDH (ABS16, Millipore, Billerica, MA).

Histology

Mice were intracardially perfused with 4% paraformaldehyde in phosphate buffered saline (PBS). Brains were removed and postfixed overnight in 4% paraformaldehyde in PBS and subsequently cryoprotected in 30% sucrose solution in PBS, snap frozen and stored at -80 °C until required. Coronal brain sections (25 μm thick) were cut on a cryostat (LEICA CM1900, Wetzlar, Germany) and mounted on gelatin-coated glass slides. Nissl staining was performed according to standard protocols. Sections were cover slipped using Poly-Mount (Polysciences Inc. Boston, MA). Fluoro Jade C (FJC) staining was performed according to the manufacturer's instruction [Ready-to-Dilute (RTD) Fluoro-Jade C Staining Kit, Biosensis, CA] [8]. Slides were incubated in sodium hydroxide for 5 min, then washed with 70% EtOH followed by distilled water. Slides were then incubated in potassium permanganate for 10 min. Next, slides were washed with distilled water and moved to low-light for staining with FJC and 4, 6-diamidino-2-phenylindole (DAPI) for 15 min. Slides were rinsed with distilled water, and cleared by brief immersion in xylenes. Slides were then coverslipped using DPX (Merck KGaA, Darmstadt, Germany).

For immunohistochemistry, sections were incubated for 1 h in a blocking buffer (PBS 5% BSA, 0.1% Polyoxyethylene Sorbitan Monolaurate) and incubated with the primary antibody (anti-Ki67), at 4 °C overnight, followed by incubation for 1 h with secondary antibody polymer solution conjugated with anti-rabbit IgG secondary antibodies and horse-radish peroxidase (Envision + System, Dako, Glostrup, Denmark). Ki67 positive cells in dentate gyrus were counted. For immunofluorescence, sections were incubated with the primary antibodies (anti-Iba-1 and anti-DCX) after blocking, at 4 °C overnight, followed by incubation for 1 h with secondary antibody (Cy3-conjugated AffiniPure goat anti-Rabbit IgG; 1 : 500, Jackson ImmunoReseach, inc. PA) in the dark at 25 °C. Sections were cover slipped using DPX. Sections

were photographed at 40 × magnification and images were captures using a KEYENCE BZ-X710 microscope (Keyence Corporation, Osaka, Japan). Iba-1 positive cell in the hippocampus, CA1, and CA3, and DCX positive cells in the dentate gyrus were counted, and densities (counts/mm^2) calculated.

Measurements of hippocampal and cortical volume

Serial coronal brain slices were cut at a thickness of 25 μm using a cryostat. H&E staining was performed according to standard protocols. Areas of the left hippocampus and cortex (primary somatosensory cortex, motor cortex, and insular cortex) were measured in every 100 μm that contained whole hippocampus and cortex using a KEYENCE BZ-X710 microscope. These area (mm^2) × 0.1 (mm) from all sections were summed and recorded as a unilateral hippocampal and cortical volume (mm^3) [9]. Relative values of hippocampal and cortical volume were represented as a percentage of average volume of control mice.

Western Blotting

Brain tissues and primary cell cultures were homogenized on ice in RIPA [50 mM Tris–HCl pH 8.0, 150 mM NaCl, 5 mM ethylenediaminetetraacetic acid (EDTA), 1% NP-40, 0.1% sodium dodecyl sulfate (SDS), 0.5% deoxycholate (DOC)] buffer containing 1 : 1000 dilution of a protease inhibitor cocktail (CalBiochem, San Diego, CA, USA) with a tissue homogenizer (Brinkmann Instruments, Westbury, NY, USA). Protein concentrations were determined using a BCA protein assay kit (Nacalai tesque, Tokyo, Japan). 10 μg protein/lane of lysates was subjected to SDS-polyacrylamide gel electrophoresis and transferred to nitrocellulose membranes (Bio-Rad, Redmond, WA). After blocking with 5% skim milk (MEGMILK SNOW BRAND Co Ltd, Tokyo, Japan) in PBS containing 0.05% Tween 20 (PBS-T), the membranes were incubated with the primary antibodies overnight, followed by incubation with horseradish peroxidase-conjugated secondary antibodies (Cell Signaling Technology, Beverly, MA) and washing with PBS-T three times. The membranes were treated with reagent for exposure (Chemi-Lumi One Super, Nacalai tesque, Tokyo, Japan; ImmunoStar LD, Wako, Japan). Image of the membranes was captured using a C-DiGit blot scanner (LI-COR, Lincoln, NE) and subjected to ImageJ analysis. Each membrane was probed with only 1 antibody, with α-tubulin or GAPDH used as a loading control.

ELISA analysis

Total lipids were extracted using n-hexane/2-propanol (3:2, by vol, HIP). The HIP was added to hippocampal tissue. Samples were homogenized at maximum speed. The homogenate was centrifuged at 1500 × *g* for 10 min at room temperature. The supernatant fraction was decanted and being dried down using an integrated SpeedVac® concentrator (SPD111V, Thermo Scientific, Rockford, IL, USA). The fraction was diluted 500 μl in assay buffer. The PGD_2, PGE_2, and $PGF_{2\alpha}$ concentration was assayed with each EIA kit (Cayman Chemicals, Ann Arbor, MI).

The WT and GPR120 KO mice were fasted overnight. For plasma GLP-1 quantification, blood samples were collected in test tubes containing a sitagliptin (100 μM) and then centrifuged for 20 min at 1,200 × *g*

at 4 °C. Intestinal and intracerebral GLP-1 was extracted according to the method by Cani *et al* [23] and McClean *et al* [24], respectively. The acid ethanol (75% ethanol + 0.15 mol/L hydrochloric acid) was added to intestinal and brain tissue. Samples were homogenized at maximum speed and placed at 4 °C for 24 h. The homogenate was centrifuged at 5000 × *g* for 20 min at 4 °C. The supernatant fraction was decanted and being dried down using an integrated SpeedVac® concentrator. The active GLP-1 concentration was assayed with Active GLP-1 ELISA Kit (FUJIFILM, Gunma, Japan). Results were measured in a Benchmark Microplate Reader (Bio-Rad, Redmond, WA).

RNA extraction and quantitative real-time PCR (Q-PCR)

Tissue samples and neuronal and glial primary cell cultures were processed for RNA extraction using ISOGEN (NIPPON GENE, Tokyo, Japan) following the manufacturer's instructions. RNA was reverse transcribed using PrimeScript RT reagent kit (TAKARA BIO INC, Shiga, Japan) reverse transcriptase. Q-PCR was performed using the Quant Studio 12K Flex (Applied Biosystems, CA). The following primer sequences were used: Phosphoglycerate kinase 1 (*PGK1*; Forward: 5'-tgctgttccaagcatcaaa-3' Reverse: 5'-gcatcttttcccttcccttc-3'); *GPR120* (Forward: 5'-gtcgtctgccacctgctctt-3' Reverse: 5'-tttctcctatgcggttgggc-3'); *NeuN* (Forward: 5'-agcagcccaaacgactacat-3' Reverse: 5'- acaagagagtggtgggaacg-3'); *GFAP* (Forward: 5'-gcttcctggaacagcaaaac-3' Reverse: 5'-cggcgatagtcgttagcttc-3'); *Iba-1* (Forward: 5'-gaagcgaatgctggagaaac-3' Reverse: 5'-gaccagttggcctcttgtgt-3'); *SOD2* (Forward: 5'-ggccaagggagatgttacaa-3' Reverse: 5'-gaaccttggactcccacaga-3'); *14-3-3ζ* (Forward: 5'-cccattcgtttaggtcttgc-3' Reverse: 5'-cctgcagcgcttctttattc-3'); *COX-1* (Forward: 5'-cagtgcctcaaccccatagt-3' Reverse: 5'-gtggctatttcctgcagctc-3'); *COX-2* (Forward: 5'-ccccaaagatagcatctgga-3' Reverse: 5'-gctgtacaagcatggcaaa-3'); *L-PGDS* (Forward: 5'-catagttggccaccact-3' Reverse: 5'-tccgggagaagaaagctgta-3'); *H-PGDS* (Forward: 5'-cgaggtgcttgatgtgtgag-3' Reverse: 5'-tgttttggaggtggaaggac-3'); *GLP-1 receptor* (Forward: 5'-ccaggttccttcgtgaatgt-3' Reverse: 5'-caaggcggagaaagaaagtg).

Behavioral tests

The Y maze apparatus (Hazai-ya, Tokyo, Japan) was a 3-arm radial maze with equal angles between all arms (8 cm width) and a bottom with 40 cm (length) and 15 cm height. Mice were tested individually by placing them in an arm of the maze and allowing them to move freely throughout the 3 different arms for 10 min. The sequence and entries into each arm were recorded. An alternation was determined from successive consecutive entries into the 3 different arms on overlapping triads in which all arms were represented. For example, ACBABCABAB, a sequence of entries to the 3 arms A, B, or C, would generate 5 ‘successful’ alternations, ACB, CBA, ABC, BCA, and CAB; the total number of possible alternations corresponded to the number of the total arm entries minus 2 (in this example, the total number would equal 8). The percentage alternation was calculated as (the number of ‘successful’ alternations divided by the number of the total arm entries minus 2) × 100. We analyzed the percentage alternation and the total number of arm entries.

Morris water maze consisted of circular pool (diameter, 150 cm; height, 40 cm) was divided into four quadrants (north, east, west, and south) and at the center of the north quadrant, a platform was placed.

The geometric shapes were pasted at the walls for visual cues. A 10 cm transparent platform was placed 1 cm beneath the surface of the water and 40 cm from the wall in the South-West quadrant of the pool. Mice were placed in a quadrant and given time to find the platform in 90 seconds during the first five days (escape latency). If the animal did not find the platform at the set time, it handler directed to the platform in training. The next five days, the platform was removed, the amount of time the mice spends in proximity to its former location is gauged (known as a probe trial) to assess memory. The mice were allowed 300 seconds to swim in order to evaluate their reference memory (cross-platform time). Mice were video tracked and analyzed behavioral parameters.

Cell cultures

Primary cell cultures were separately following the method [25]. Primary neurons were prepared from cerebral cortex of embryonic day 18 mouse embryo. Brains were stripped of meninges and dissected from diencephalon, were dispersed and incubated at 37 °C in Hank's balanced salt solution (HBSS) containing 0.25% trypsin (Life Technologies, CA) and 0.001% DNase I (Roche Diagnostics, Mannheim, Germany). After inhibiting the trypsin with fetal bovine serum, the suspension was again disrupted with a pipette and filtered through a 70 μm nylon mesh (BD Falcon, MA). The filtered cell suspension was placed in poly-L-lysine-coated 75 cm^2 flasks and kept at 37 °C in a humidified incubator with 5% CO_2 in air. Neuronal cells were cultured in Neurobasal Medium (Life Technologies, CA) with B27 supplement. After 1 day, the medium was replaced with Neurobasal Medium. The culture medium was subsequently changed twice a week. Cells were harvested after 14 days *in vitro*.

Primary mixed glial cultures (astrocytes and microglia) were prepared from forebrains of postnatal 2 days old mice using a differential detachment method [26, 27]. Briefly, forebrains free of meninges were digested with HBSS containing 0.25% trypsin and 0.001% DNase I and triturated with DMEM containing 10% heat-inactivated fetal bovine serum and 1% penicillin–streptomycin. Dissociated cells were plated in poly-L-lysine-coated 75 cm^2 flasks. The culture medium was changed twice a week. Astrocytes were detached from the 75 cm^2 flasks by trypsinization. Individual glial cells were used for the experiments. After 14 days *in vitro*, when cultures reached a confluence, microglia were isolated by shaking the mixed glia-containing flasks for 1 h at 200 rpm and plated with 500,000 cells/ well in 6-well plates. After resting for 24 h, microglia were stimulated with 100 ng/ml Lipopolysaccharide (LPS, Sigma, Deisen-hofen, Germany) 1 h after pretreatment with 10 ng/ml liraglutide. In the PGD_2 addition experiment, microglia were incubated with the medium containing rat recombinant GM-CSF (20 ng/mL, Pepro Tech, London, UK) after plated with 500,000 cells/well. After resting for 24 h, cells stimulated with 1 μM PGD_2 (Cayman CHEMICAL, Ann Arbor, MI) 1 h after pretreatment with 1 μM MK-0524 (DP1 antagonist, Axon MEDCHEM, Groningen, Netherlands), 1 μM OC459 (DP2 antagonist, Axon MEDCHEM, Groningen, Netherlands). The isolated primary cells with each isolation method were determined by PCR using NeuN, GFAP, and Iba-1 primers (Additional file 1: Fig. S1B).

Statistics

Two-sample comparisons were carried out using a student's *t*-test. Multiple comparisons were performed by one-way ANOVA followed by Newman-Keuls post-hoc test or two-way ANOVA followed by post-hoc Tukey test. Graph Pad Prism Ver. 5.01 (Graph Pad Software, Inc., San Diego, CA) and expressed as mean ± SEM. p values < 0.05 were considered statistically significant.

Results

To investigate the contribution of GPR120 on neuronal function, we measured unilateral cortical and hippocampal volume of WT and GPR120 KO mice. Although no statistically significant difference was observed in cortical volume (Fig. 1A), a statistically significant hippocampus-specific decline in tissue volume was observed in GPR120 KO mice (Fig. 1B). To investigate detailed hippocampal structure, we counted pyramidal neurons in Nissl-stained sections of CA1, CA2, and CA3. The number of Nissl positive cells in the hippocampus of GPR120 KO mice was significantly decreased compared with that of WT mice (Fig. 1C), particularly in CA3 (Fig. 1D and E) and CA1 (Additional file 1: Fig. S1C and D), but not in CA2 (Additional file 1: Fig. S1C and E). Neither GPR120 KO nor WT mice exhibited any sign of neuronal death in the hippocampus, as determined by FJC staining, a specific staining for degenerative neurons (Additional file 1: Fig. S1F). Although numerous FJC-positive neurons were detected in the WT hippocampus after kainic acid (KA)-induced excitotoxicity, they were hardly detectable in the GPR120 KO hippocampus (Additional file 1: Fig. S1F). Therefore, reduced hippocampal volume in GPR120 KO mice was considered to be independent from neuronal death.

Neurogenesis is an important contributor to hippocampal volume and structure [28, 29]. The dentate gyrus is the hippocampal region where life-long neurogenesis occurs [30]. To evaluate neurogenesis in the hippocampus, we examined expression levels of DCX and Ki67, which are neurogenesis markers [31]. The decreased hippocampal DCX protein levels (Fig. 1F and G) and DCX positive cells (Fig. 1H and I) revealed reduced neurogenesis in the GPR120 KO hippocampus. Similarly, the frequency of Ki67-positive cells in the dentate gyrus of GPR120 KO mice was markedly lower than that in WT mice (Fig. 1J and K). SOD2 and 14-3-3z expressions play an important role in neurogenesis [32, 33]. The expression levels of both SOD2 and 14-3-3z significantly reduced in the GPR120 KO hippocampus (Fig. 1F, L, and M) (Additional file 1: Fig. S1G and H).

Reduced hippocampal volume is associated with cognitive decline in neuronal disorders [34, 35, 36]. We therefore examined synaptic protein expression levels and conducted behavioral tests of working memory and spatial learning. The expression of the presynaptic protein synaptophysin (Fig. 1F and N) and the postsynaptic protein PSD95 (Fig. 1F and O) were reduced in the GPR120 KO hippocampus. Y-maze spontaneous alternation test results indicated that GPR120 KO mice had an impaired working memory (Fig. 1P). Two sets of Morris water maze trial were used to evaluate spatial reference memory - place trials (submerged platform) and probe trials (removed platform). In the place trials, the escape latency time of GPR120 KO mice was longer than that of WT mice (Fig. 1Q). Furthermore, the cross-platform time of GPR120 KO mice was shorter than that of WT mice in the probe test (Fig. 1R). These results indicated cognitive decline in GPR120 KO mice. Taken together, GPR120 KO mice exhibited

various symptoms of neurodegeneration: declines in hippocampal volume, hippocampal cell number, neurogenesis, and cognitive function.

Considering that microglial-activation-induced neuroinflammation can be a causative factor of neurodegeneration in GPR120 KO mice, we examined microglial activation in the hippocampus by measuring Iba-1 expression levels. There was an upregulation of Iba-1 mRNA (Additional file 2: Fig. S2A) and protein (Fig. 2A and B) in the hippocampus of GPR120 KO mice, corresponding to the increase in the number of Iba-1-positive microglia in the CA1 (Additional file 2: Fig. S2B and C), CA3 (Fig. 2C and D), and hippocampus (Fig. 2E) of GPR120 KO mice. Although astrocytes also react to neuroinflammation by upregulating GFAP expression, which results in astrogliosis [37], no significant difference was observed in GFAP protein levels between WT and GPR120 KO hippocampus (Fig. 2A and F).

Previously we demonstrated that a surge in PGD_2 production enhanced persistent microglial activation in the hippocampus after KA-induced excitotoxicity [8, 9]. In the present study, we revealed an increase in hippocampal PGD_2 production in intact GPR120 KO mice without KA administration, which was almost comparable in concentration to that in the hippocampus of WT mice with KA administration (Fig. 2G). PGE_2 and $PGF_{2\alpha}$ productions remained unchanged in the GPR120 KO hippocampus (Fig. 2G). PGD_2 levels were slightly elevated in various organs of GPR120 KO mice compared with WT mice, but PGD_2 levels were not elevated in the cortex (Fig. 2H). To investigate which enzymes were responsible for PGD_2 production in the GPR120 KO hippocampus, we measured the protein expression levels of PGD_2 synthesis enzymes, COX-1, COX-2, L-PGDS, and H-PGDS (Fig. 2I-L). COX-1, COX-2, and H-PGDS protein levels were higher in the GPR120 KO hippocampus than in the WT hippocampus (Fig. 2I-L). The expression levels of genes encoding these enzymes were also higher in the GPR120 KO hippocampus than in the WT hippocampus (Additional file 2: Fig. S2D-G). Especially notable were the upregulations of H-PGDS gene and protein expressions (Fig. 2L and Additional file 2: Fig. S2G). These results suggest that the hippocampus of GPR120 KO mice exhibited constant neuroinflammation, as characterized by increased PGD_2 production and microglial activation.

To elucidate whether elevated PGD_2 production was associated with hippocampal neurodegeneration in GPR120 KO mice, we treated mice with indomethacin to suppress PGD_2 production via inhibition of COXs. Similar to our previous results [10], indomethacin treatment almost completely inhibited hippocampal PGD_2 production in both groups of mice (Fig. 3A). H-PGDS protein levels in the GPR120 KO hippocampus decreased upon inhibition of PGD_2 production (Fig. 3B and C). Inhibition of PGD_2 production did not affect GFAP protein levels in both groups of mice (Fig. 3B and Additional file 3: Fig. S3A). The reduction in PGD_2 production also reduced Iba-1 protein levels (Fig. 3B and D) and Iba-1 positive microglia in the hippocampus of GPR120 KO and WT mice (Fig. 3E-G and Additional file 3: Fig. S3B and C). These data suggest that hippocampal PGD_2 production was the cause of the microglial activation observed in the GPR120 KO hippocampus. Moreover, inhibition of PGD_2 production increased DCX protein levels (Fig. 3B and H), DCX-positive cells (Fig. 3I and J), and expression levels of SOD2 (Fig. 3B, K and L) and 14-3-3z (Additional file 3: Fig. S3D and E) in the hippocampus *of GPR120 KO* mice.

Furthermore, inhibition of PGD_2 production significantly attenuated the reduction of hippocampal volume in GPR120 KO mice (Fig. 3M), but did not affect cortical volume in mice of either group (Fig. 3N). The synaptic proteins, synaptophysin and PSD95, were increased by inhibition of PGD_2 production in GPR120 KO mice (Fig. 3B, O and P). Taken together, inhibition of PGD_2 production attenuated the decline in neurogenesis, hippocampal volume, and synaptic protein levels in the hippocampus of GPR120 KO mice.

To investigate which cell types could produce PGD_2 in the hippocampus, we examined gene expression levels of PGD_2 synthesis enzymes in primary neurons, astrocytes, and microglia (Fig. 4A-D). COX-1 and H-PGDS were mainly expressed in microglia (Fig. 4A and D), COX-2 was mainly expressed in neurons (Fig. 4B), and L-PGDS exhibited similar expression levels in all three cell types (Fig. 4C). These results suggested that microglia are major producers of PGD_2, which is in agreement with previous reports [38]. We also demonstrated that PGD_2 addition increased microglial Iba-1 levels, which was attenuated by DP1 and DP2 antagonists (Fig. 4E), suggesting that microglial activation via PGD_2 was in an autocrine manner.

Tissue distribution analyses were performed by real-time PCR to investigate which tissue expressed GPR120, in order to further elucidate the mechanism leading to the observed neurological phenotypes in GPR120 KO mice. There was abundant expression of GPR120 mRNA in the small intestine, colon, and adipose tissues (Fig. 5A), however, we could not detect GPR120 mRNA in the whole brain, hippocampus, or cortex. Our data are in agreement with studies demonstrating the tissue specific expression of GPR120 [11, 39]. To investigate the peripheral and intracerebral levels of GLP-1, an incretin that is secreted via PUFA/GPR120 signaling [11], we measured intestinal, plasma, and intracerebral GLP-1 levels under fasting and fed states. Although we observed dietary elevation of intestine, plasma, and intracerebral GLP-1 levels in WT mice, no such elevation was observed in GPR120 KO mice (Fig. 5B-D). The intestinal, plasma, and intracerebral GLP-1 levels in GPR120 KO mice were lower than that in WT mice during fed states (Fig. 5B-D). To investigate whether GLP-1 bioactivity directly affected microglial PGD_2 production, we added a GLP-1 analogue, liraglutide, to primary microglial cell cultures. PGD_2 production and H-PGDS mRNA expression increased in the LPS-stimulated primary microglia and decreased upon liraglutide addition (Fig. 5E and F). The expressions of GLP-1 receptor mRNA were detected in not only the small intestine, but also hippocampal tissue and primary microglia (Fig. 5G). These data indicated that GLP-1 bioactivity directly reduced PGD_2 production in microglia.

To elucidate the relationship between peripheral GLP-1 levels and neurological phenotypes, we attempted to potentiate peripheral GLP-1 bioactivity in GPR120 KO mice. Oral administration of sitagliptin, an inhibitor of dipeptidyl peptidase-4 (DPP-4), an enzyme that degrades GLP-1, reduced PGD_2 production in the GPR120 KO hippocampus (Additional file 4: Fig. S4A). Peritoneal treatment with liraglutide reduced PGD_2 production (Fig. 6A) and H-PGDS protein levels (Fig. 6B and C) in GPR120 KO hippocampus. Although liraglutide treatment did not affect GFAP protein levels (Fig. 6B and Additional file 4: Fig. S4B), Iba-1 gene (Additional file 4: Fig. S4C) and protein levels (Fig. 6B and D) and Iba-1 positive microglia (Fig. 6E-G and Additional file 4: Fig. S4D and E) were reduced by liraglutide. These results suggested that

potentiation of peripheral GLP-1 bioactivity led to a decrease in PGD_2 production and microglial activation in the GPR120 KO hippocampus. Moreover, peritoneal treatment with liraglutide increased hippocampal DCX protein levels (Fig. 6B and H), DCX-positive cells (Fig. 6I and J), expression levels of SOD2 (Fig. 6K and L) and 14-3-3z (Additional file 4: Fig. S4F and G), and synaptophysin and PSD95 protein levels (Fig. 6B, N and O), and attenuated the reduction of hippocampal volume (Fig. 6M) in GPR120 KO mice. Furthermore, treatment with liraglutide improved behavioral outcomes as measured in the Y-maze (Fig. 6P) and the Morris water maze tests (Fig. 6Q and R), indicating that cognitive decline in GPR120 KO mice was ameliorated by this treatment. These results suggest that potentiation of peripheral GLP-1 bioactivity prevented neurodegeneration in GPR120 KO mice.

Discussion

In the current study, to reveal the relationship between PGD_2-microglia-provoked neuroinflammation and intestinal PUFA/GPR120 signaling, we performed neurological analysis of GPR120 KO mice. We revealed notable neuroinflammation (PGD_2 overproduction and microglial hyperactivation) and neurodegeneration (declines in neurogenesis, hippocampal volume, and cognitive function) in GPR120 KO mice. We also demonstrated that inhibition of PGD_2 production attenuated PGD_2-microglia-provoked neuroinflammation. Furthermore, the potentiation of peripheral GLP-1 bioactivity in the form of a GLP-1 analogue, liraglutide, in GPR120 KO mice prevented neuroinflammation and neurodegeneration. These results indicated that PGD_2-microglia-provoked neuroinflammation triggered the neurodegeneration observed in GPR120 KO mice, which could be suppressed by an increase in peripheral GLP-1 bioactivity. In addition, GPR120 mRNA was expressed in intestinal tissues, but we did not detect it in brain tissues (the whole brain, the cortex, or the hippocampus). Our data are in agreement with studies that have demonstrated tissue-specific expression of GPR120 [11, 13]. These results indicate that neuroinflammation and neurodegeneration observed in GPR120 KO mice are probably caused by defects in intestinal GPR120 function and not in the CNS. Therefore, we focused on the incretin, GLP-1, as it is secreted via intestinal PUFA/GPR120 signaling [11], cross BBB [16], and increases neuronal activities [19]. Taken together with the reduced GLP-1 levels in the intestine and plasma of GPR120 KO mice, their neurological phenotypes were caused by the decline of intracerebral GLP-1 levels, which was caused in turn by insufficient GLP-1 secretion from GPR120 signaling-defective intestine and low entry of GLP-1 into the brain (Fig. 7). In the GPR120 KO hippocampus, increased PGD_2 production downregulated SOD2 expression, which would fail to scavenge reactive oxygen species (ROS), a leading cause of reduced neurogenesis. Thus, intestinal GLP-1 bioactivity by GPR120 stimulation may remotely contribute to hippocampal homeostasis via suppression of PGD_2-microglia-provoked neuroinflammation (Fig. 7).

We considered that PGD_2-microglia-provoked neuroinflammation was the main cause of neurodegeneration observed in GPR120 KO mice. Our *in vitro* experiments with primary microglial cell cultures revealed that H-PGDS expression increased PGD_2 production and microglial Iba-1 expression, which could be blocked by DP1- and DP2-antagonists. These data suggest that microglia were activated by PGD_2 in an autocrine manner. An upregulation of hippocampal PGD_2 in GPR120 KO mice was

observed even without KA-administration, at a level that was almost equal to that in the hippocampus of KA-administrated WT mice. Constant PGD_2-induced microglial activation results in neuroinflammation in the hippocampus of GPR120 KO mice without external stimulation. Previously we reported a surge in PGD_2 production in the hippocampus of KA-administrated WT mice [10], which led to PGD_2-enhanced persistent microglial activation [8, 9]. Excessive microglial activation plays a pivotal role in neuroinflammation and causes neurodegeneration by inhibiting neurogenesis via the secretion of ROS [40, 41, 42]. Previous study reported that SOD2 KO mice exhibited reduced neurogenesis [43], indicating that scavenging of ROS by SOD2 plays an important role in neurogenesis. In our results, microglial PGD_2 production downregulated SOD2 expression, suggesting that PGD_2-microglia-provoked neuroinflammation could lead to the neurodegeneration via inhibition of neurogenesis in GPR120 KO hippocampus. In addition to SOD2, 14-3-3ζ protein also affects neurogenesis through regulation of neuronal differentiation into neurons [33] and its expressions was reduced by microglial PGD_2 production. Thus, microglial PGD_2 production inhibited neurogenesis via suppression of SOD2 and 14-3-3ζ expressions, which is in agreement with a study of Alzheimer's disease mice model [44]. We observed this neuroinflammatory pathway specifically in the hippocampus. One possible reason may be the potential ability of the hippocampus to produce PGD_2. We previously reported that KA-induced elevation of PGD_2 production was observed in the hippocampus, and not in the cortex [10], suggesting that this pathway was activated specifically in the hippocampus, probably due to its higher ability to produce PGD_2.

We observed declines in neurogenesis, hippocampal volume, and cognitive function in GPR120 KO mice in the present study. There is an important association among these neurological phenotypes. It is well known that cognitive decline in Alzheimer's disease and type 2 diabetes mellitus are correlated with a decrease in hippocampal volume [45, 46]. A genome-wide association analysis conducted as part of the Alzheimer's disease Neuroimaging Initiative revealed a significant relationship between neurogenesis and hippocampal volume in humans [19]. Further, the main GLP-1 degrading enzyme, DPP-4, is associated with hippocampal volume, suggesting that insufficient GLP-1 levels may also be related to hippocampal volume [29]. These observations suggest that insufficient GLP-1 level may contribute to neurodegeneration in neuronal diseases exhibiting cognitive impairment.

In our results, GPR120 KO mice showed reduced intestinal, plasma, and intracerebral GLP-1 levels, suggested that an insufficiency of intestinal GLP-1 secretion could be a cause of decline in intracerebral GLP-1 levels. Supporting this concept, GLP-1 is known to be secreted from intestinal enteroendocrine L cells and can act on other organs via systemic circulation [47]. Since sitagliptin, an inhibitor of DPP-4, does not cross the BBB [48], it can inhibit the degradation of peripheral GLP-1, but not of intracerebral GLP-1. Previous study reported that oral administration of sitagliptin enhances intracerebral GLP-1 levels [49], indicates that elevation of peripheral GLP-1 levels raises the intracerebral GLP-1 level via the blood stream. In the present study, we showed that oral administration of sitagliptin reduced hippocampal PGD_2 production in GPR120 KO mice (Additional file 4: Fig. S4A). Also, we demonstrated that GLP-1 receptor was expressed in microglia, GLP-1 bioactivity reduced microglial activation, and microglia were

the main cells to produce PGD_2 in the brain. Taken together, these observations suggest that intestinal GLP-1, secreted by intestinal GPR120 stimulation, and transported via the bloodstream, acts remotely on microglia by reducing microglial PGD_2 production.

In this study, dietary elevation of GLP-1 levels was not observed in GPR120 KO mice. We previously reported that GPR120 senses and responds to several PUFA [11, 12], including two of most abundant PUFA in the brain: AA and DHA [50, 51]. AA and DHA metabolisms are critical to brain development and maintenance of brain structure. Our results suggest that intestinal PUFA/GPR120 signaling prevent neurodegeneration via suppression of PGD_2-microglia-provoked neuroinflammation. Thus, to sense and detect these key PUFA, such as AA and DHA, by GPR120 might be an important strategy for keeping hippocampal homeostasis.

Conclusion

In the current study, we revealed that dysfunction of GPR120 caused PGD_2 overproduction, persistent microglial activation, loss of neurogenesis, decreased hippocampal volume, and cognitive decline. Specifically, insufficient GLP-1 bioactivity was a result of GPR120 dysfunction, and induced PGD_2-microglia-provoked neuroinflammation, which is a major factor of the neurodegeneration observed in GPR120 KO mice. These findings may suggest that insensitivity to dietary PUFA by dysfunction of GPR120 would raise the risk of hippocampal dysfunction. These observations may reveal the presence of a novel gut-brain interaction, in that the signaling of dietary PUFA is sensed by GPR120, converted into incretin bioactivity, and contributes to hippocampal homeostasis via suppression of PGD_2-microglia-provoked neuroinflammation. Furthermore, our results illustrated that potentiation of GLP-1 bioactivity suppressed this neuroinflammatory pathway, indicating a potentially novel mechanism of action for incretin-based therapies, which are promising treatment options for cognitive decline in patient with Alzheimer's disease and type 2 diabetes mellitus.

List Of Abbreviations

AA: arachidonic acid, COX: cyclooxygenase, DCX: doublecortin, DHA: docosahexaenoic acid, DPP-4: dipeptidyl peptidase-4, FJC: Fluoro Jade C, GFAP: glial fibrillary acidic protein, GLP-1: glucagon-like peptide-1, H-PGDS: hematopoietic prostaglandin D synthase, Iba-1: ionized calcium binding adapter molecule 1, KA: kainic acid, KO: knockout, Lira: liraglutide, L-PGDS: lipocalin-type prostaglandin D synthase, LPS: lipopolysaccharide, PG = prostaglandin, PSD95: postsynaptic density protein 95, PUFA: polyunsaturated fatty acids, ROS: reactive oxygen species, SOD: superoxide dismutase, WT: wild-type

Declarations

Ethics approval and consent to participate

All animal studies were approved by the **Institutional Animal Care and Use Committee** and DNA experiment Safety Committee of Saitama Medical University.

Consent for publication

Not applicable.

Availability of data and materials

Not applicable.

Competing interests

The authors declare that they have no competing interests.

Funding

This research was supported by MEXT KAKENHI (Grant Number 18K06899, 18K17933, 18K07354, and 25870677), Food Science Institute Foundation (Ryoushoku-kenkyukai, Kanagawa, Japan), Towa Foundation for Food Research, Public health research foundation, Mishima Kaiun Memorial Foundation, and Saitama Medical University internal grant (17-B-1-23, 19-A-1-01).

Authors' contributions

KI performed the majority of experiments. SY, KoY, and CS performed experiments, contributed data. TA, KM, AH, and KeY designed the research study. KI and KeY wrote the first draft of the manuscript. SY, NY, TA, KM, YT, and AH contributed to the writing of the manuscript. KM and AH supervised the entire project and reviewed the manuscript. All authors read and approved the final manuscript.

Acknowledgements

We greatly appreciate the valuable comments and suggestions from D Hishikawa, K Yanagida, M Ishikawa, N Ueno, S Suo, and S Yagishita. The authors thank the Division of Laboratory Animal Medicine, Biomedical Research Center, Saitama Medical University, for maintaining the mice. We thank Messrs. A Sasaya, A Suzuki, M Noguchi, R Suzuki, N Takagi, S Nemoto, H Oda, M Sato, N Ishikawa, K Ichijo, N Eguchi, E Furukawa, Y Kataoka, and M Nihei (Saitama Medical University Faculty of Health and Medical) for research support.

References

1. Vezzani A, Balosso S, Ravizza T: **Neuroinflammatory pathways as treatment targets and biomarkers in epilepsy.** *Nature reviews Neurology* 2019, **15:**459-472.
2. Seo MJ, Oh DK: **Prostaglandin synthases: Molecular characterization and involvement in prostaglandin biosynthesis.** *Progress in lipid research* 2017, **66:**50-68.

3. Santini G, Mores N, Malerba M, Mondino C, Macis G, Montuschi P: **Investigational prostaglandin D2 receptor antagonists for airway inflammation.** *Expert opinion on investigational drugs* 2016, **25:**639-652.
4. Ransohoff RM: **How neuroinflammation contributes to neurodegeneration.** *Science (New York, NY)* 2016, **353:**777-783.
5. Colonna M, Butovsky O: **Microglia Function in the Central Nervous System During Health and Neurodegeneration.** *Annual review of immunology* 2017, **35:**441-468.
6. Kumar Sahel D, Kaira M, Raj K, Sharma S, Singh S: **Mitochondrial dysfunctioning and neuroinflammation: Recent highlights on the possible mechanisms involved in Traumatic Brain Injury.** *Neuroscience letters* 2019**:**134347.
7. Vezzani A, French J, Bartfai T, Baram TZ: **The role of inflammation in epilepsy.** *Nature reviews Neurology* 2011, **7:**31-40.
8. Iwasa K, Yamamoto S, Yagishita S, Maruyama K, Yoshikawa K: **Excitotoxicity-induced prostaglandin D2 production induces sustained microglial activation and delayed neuronal death.** *Journal of lipid research* 2017, **58:**649-655.
9. Yoshikawa K, Kita Y, Furukawa A, Kawamura N, Hasegawa-Ishii S, Chiba Y, Takei S, Maruyama K, Shimizu T, Shimada A: **Excitotoxicity-induced immediate surge in hippocampal prostanoid production has latent effects that promote chronic progressive neuronal death.** *Prostaglandins, leukotrienes, and essential fatty acids* 2013, **88:**373-381.
10. Yoshikawa K, Kita Y, Kishimoto K, Shimizu T: **Profiling of eicosanoid production in the rat hippocampus during kainic acid-induced seizure: dual phase regulation and differential involvement of COX-1 and COX-2.** *The Journal of biological chemistry* 2006, **281:**14663-14669.
11. Hirasawa A, Tsumaya K, Awaji T, Katsuma S, Adachi T, Yamada M, Sugimoto Y, Miyazaki S, Tsujimoto G: **Free fatty acids regulate gut incretin glucagon-like peptide-1 secretion through GPR120.** *Nature medicine* 2005, **11:**90-94.
12. Villegas-Comonfort S, Takei Y, Tsujimoto G, Hirasawa A, Garcia-Sainz JA: **Effects of arachidonic acid on FFA4 receptor: Signaling, phosphorylation and internalization.** *Prostaglandins, leukotrienes, and essential fatty acids* 2017, **117:**1-10.
13. Ichimura A, Hirasawa A, Poulain-Godefroy O, Bonnefond A, Hara T, Yengo L, Kimura I, Leloire A, Liu N, Iida K, et al: **Dysfunction of lipid sensor GPR120 leads to obesity in both mouse and human.** *Nature* 2012, **483:**350-354.
14. Hemmingsen B, Sonne DP, Metzendorf MI, Richter B: **Dipeptidyl-peptidase (DPP)-4 inhibitors and glucagon-like peptide (GLP)-1 analogues for prevention or delay of type 2 diabetes mellitus and its associated complications in people at increased risk for the development of type 2 diabetes mellitus.** *The Cochrane database of systematic reviews* 2017, **5:**Cd012204.
15. Davies M, Speight J: **Patient-reported outcomes in trials of incretin-based therapies in patients with type 2 diabetes mellitus.** *Diabetes, obesity & metabolism* 2012, **14:**882-892.

16. Kanoski SE, Hayes MR, Skibicka KP: **GLP-1 and weight loss: unraveling the diverse neural circuitry.** *American journal of physiology Regulatory, integrative and comparative physiology* 2016, **310:**R885-895.
17. Hamilton A, Holscher C: **Receptors for the incretin glucagon-like peptide-1 are expressed on neurons in the central nervous system.** *Neuroreport* 2009, **20:**1161-1166.
18. Bomba M, Granzotto A, Castelli V, Massetti N, Silvestri E, Canzoniero LMT, Cimini A, Sensi SL: **Exenatide exerts cognitive effects by modulating the BDNF-TrkB neurotrophic axis in adult mice.** *Neurobiology of aging* 2018, **64:**33-43.
19. During MJ, Cao L, Zuzga DS, Francis JS, Fitzsimons HL, Jiao X, Bland RJ, Klugmann M, Banks WA, Drucker DJ, Haile CN: **Glucagon-like peptide-1 receptor is involved in learning and neuroprotection.** *Nature medicine* 2003, **9:**1173-1179.
20. Suemizu H, Yagihashi C, Mizushima T, Ogura T, Etoh T, Kawai K, Ito M: **Establishing EGFP congenic mice in a NOD/Shi-scid IL2Rg(null) (NOG) genetic background using a marker-assisted selection protocol (MASP).** *Experimental animals* 2008, **57:**471-477.
21. Kamble M, Gupta R, Rehan HS, Gupta LK: **Neurobehavioral effects of liraglutide and sitagliptin in experimental models.** *European journal of pharmacology* 2016, **774:**64-70.
22. DellaValle B, Brix GS, Brock B, Gejl M, Rungby J, Larsen A: **Oral Administration of Sitagliptin Activates CREB and Is Neuroprotective in Murine Model of Brain Trauma.** *Frontiers in pharmacology* 2016, **7:**450.
23. Cani PD, Dewever C, Delzenne NM: **Inulin-type fructans modulate gastrointestinal peptides involved in appetite regulation (glucagon-like peptide-1 and ghrelin) in rats.** *The British journal of nutrition* 2004, **92:**521-526.
24. McClean PL, Parthsarathy V, Faivre E, Hölscher C: **The diabetes drug liraglutide prevents degenerative processes in a mouse model of Alzheimer's disease.** *The Journal of neuroscience : the official journal of the Society for Neuroscience* 2011, **31:**6587-6594.
25. Iwasa K, Yamamoto S, Takahashi M, Suzuki S, Yagishita S, Awaji T, Maruyama K, Yoshikawa K: **Prostaglandin F2alpha FP receptor inhibitor reduces demyelination and motor dysfunction in a cuprizone-induced multiple sclerosis mouse model.** *Prostaglandins, leukotrienes, and essential fatty acids* 2014, **91:**175-182.
26. Li J, Ramenaden ER, Peng J, Koito H, Volpe JJ, Rosenberg PA: **Tumor necrosis factor alpha mediates lipopolysaccharide-induced microglial toxicity to developing oligodendrocytes when astrocytes are present.** *The Journal of neuroscience : the official journal of the Society for Neuroscience* 2008, **28:**5321-5330.
27. Chen Y, Balasubramaniyan V, Peng J, Hurlock EC, Tallquist M, Li J, Lu QR: **Isolation and culture of rat and mouse oligodendrocyte precursor cells.** *Nature protocols* 2007, **2:**1044-1051.
28. Eisch AJ, Petrik D: **Depression and hippocampal neurogenesis: a road to remission?** *Science (New York, NY)* 2012, **338:**72-75.

29. Horgusluoglu-Moloch E, Risacher SL, Crane PK, Hibar D, Thompson PM, Saykin AJ, Nho K: **Genome-wide association analysis of hippocampal volume identifies enrichment of neurogenesis-related pathways.** *Scientific reports* 2019, **9:**14498.
30. Ming GL, Song H: **Adult neurogenesis in the mammalian brain: significant answers and significant questions.** *Neuron* 2011, **70:**687-702.
31. Whoolery CW, Walker AK, Richardson DR, Lucero MJ, Reynolds RP, Beddow DH, Clark KL, Shih HY, LeBlanc JA, Cole MG, et al: **Whole-Body Exposure to (28)Si-Radiation Dose-Dependently Disrupts Dentate Gyrus Neurogenesis and Proliferation in the Short Term and New Neuron Survival and Contextual Fear Conditioning in the Long Term.** *Radiation research* 2017, **188:**532-551.
32. Huang TT, Zou Y, Corniola R: **Oxidative stress and adult neurogenesis--effects of radiation and superoxide dismutase deficiency.** *Seminars in cell & developmental biology* 2012, **23:**738-744.
33. Toyo-oka K, Wachi T, Hunt RF, Baraban SC, Taya S, Ramshaw H, Kaibuchi K, Schwarz QP, Lopez AF, Wynshaw-Boris A: **14-3-3ε and ζ regulate neurogenesis and differentiation of neuronal progenitor cells in the developing brain.** *The Journal of neuroscience : the official journal of the Society for Neuroscience* 2014, **34:**12168-12181.
34. Dumurgier J, Hanseeuw BJ, Hatling FB, Judge KA, Schultz AP, Chhatwal JP, Blacker D, Sperling RA, Johnson KA, Hyman BT, Gomez-Isla T: **Alzheimer's Disease Biomarkers and Future Decline in Cognitive Normal Older Adults.** *Journal of Alzheimer's disease : JAD* 2017, **60:**1451-1459.
35. Van Petten C: **Relationship between hippocampal volume and memory ability in healthy individuals across the lifespan: review and meta-analysis.** *Neuropsychologia* 2004, **42:**1394-1413.
36. Elder GJ, Mactier K, Colloby SJ, Watson R, Blamire AM, O'Brien JT, Taylor JP: **The influence of hippocampal atrophy on the cognitive phenotype of dementia with Lewy bodies.** *International journal of geriatric psychiatry* 2017, **32:**1182-1189.
37. Ben Haim L, Carrillo-de Sauvage MA, Ceyzériat K, Escartin C: **Elusive roles for reactive astrocytes in neurodegenerative diseases.** *Frontiers in cellular neuroscience* 2015, **9:**278.
38. Mohri I, Eguchi N, Suzuki K, Urade Y, Taniike M: **Hematopoietic prostaglandin D synthase is expressed in microglia in the developing postnatal mouse brain.** *Glia* 2003, **42:**263-274.
39. Oh DY, Walenta E, Akiyama TE, Lagakos WS, Lackey D, Pessentheiner AR, Sasik R, Hah N, Chi TJ, Cox JM, et al: **A Gpr120-selective agonist improves insulin resistance and chronic inflammation in obese mice.** *Nature medicine* 2014, **20:**942-947.
40. Su P, Zhang J, Wang D, Zhao F, Cao Z, Aschner M, Luo W: **The role of autophagy in modulation of neuroinflammation in microglia.** *Neuroscience* 2016, **319:**155-167.
41. Kettenmann H, Kirchhoff F, Verkhratsky A: **Microglia: new roles for the synaptic stripper.** *Neuron* 2013, **77:**10-18.
42. Simpson DSA, Oliver PL: **ROS Generation in Microglia: Understanding Oxidative Stress and Inflammation in Neurodegenerative Disease.** *Antioxidants (Basel, Switzerland)* 2020, **9**.
43. Fishman K, Baure J, Zou Y, Huang TT, Andres-Mach M, Rola R, Suarez T, Acharya M, Limoli CL, Lamborn KR, Fike JR: **Radiation-induced reductions in neurogenesis are ameliorated in mice deficient**

in CuZnSOD or MnSOD. *Free radical biology & medicine* 2009, **47:**1459-1467.

44. Guo JW, Guan PP, Ding WY, Wang SL, Huang XS, Wang ZY, Wang P: **Erythrocyte membrane-encapsulated celecoxib improves the cognitive decline of Alzheimer's disease by concurrently inducing neurogenesis and reducing apoptosis in APP/PS1 transgenic mice.** *Biomaterials* 2017, **145:**106-127.
45. Dubois B, Feldman HH, Jacova C, Hampel H, Molinuevo JL, Blennow K, DeKosky ST, Gauthier S, Selkoe D, Bateman R, et al: **Advancing research diagnostic criteria for Alzheimer's disease: the IWG-2 criteria.** *The Lancet Neurology* 2014, **13:**614-629.
46. Ben Assayag E, Eldor R, Korczyn AD, Kliper E, Shenhar-Tsarfaty S, Tene O, Molad J, Shapira I, Berliner S, Volfson V, et al: **Type 2 Diabetes Mellitus and Impaired Renal Function Are Associated With Brain Alterations and Poststroke Cognitive Decline.** *Stroke* 2017, **48:**2368-2374.
47. Hou Y, Ernst SA, Heidenreich K, Williams JA: **Glucagon-like peptide-1 receptor is present in pancreatic acinar cells and regulates amylase secretion through cAMP.** *American journal of physiology Gastrointestinal and liver physiology* 2016, **310:**G26-33.
48. Chen DY, Wang SH, Mao CT, Tsai ML, Lin YS, Su FC, Chou CC, Wen MS, Wang CC, Hsieh IC, et al: **Sitagliptin After Ischemic Stroke in Type 2 Diabetic Patients: A Nationwide Cohort Study.** *Medicine* 2015, **94:**e1128.
49. Gault VA, Lennox R, Flatt PR: **Sitagliptin, a dipeptidyl peptidase-4 inhibitor, improves recognition memory, oxidative stress and hippocampal neurogenesis and upregulates key genes involved in cognitive decline.** *Diabetes, obesity & metabolism* 2015, **17:**403-413.
50. Liu JJ, Green P, John Mann J, Rapoport SI, Sublette ME: **Pathways of polyunsaturated fatty acid utilization: implications for brain function in neuropsychiatric health and disease.** *Brain research* 2015, **1597:**220-246.
51. Tassoni D, Kaur G, Weisinger RS, Sinclair AJ: **The role of eicosanoids in the brain.** *Asia Pacific journal of clinical nutrition* 2008, **17 Suppl 1:**220-228.

Figures

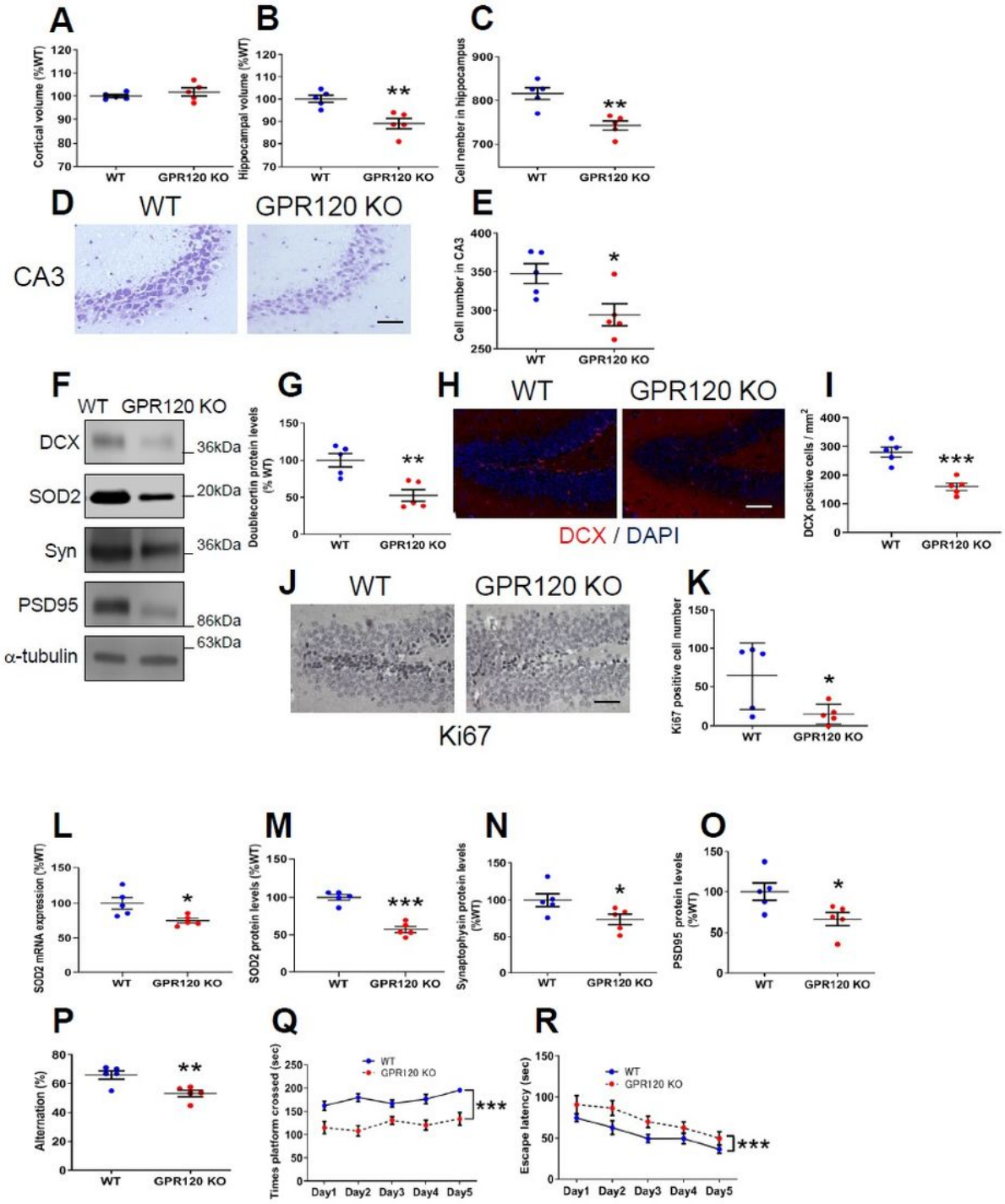

Figure 1

Declines in hippocampal volume, neurogenesis, and cognitive function observed in GPR120 KO mice. Cortical (A) and Hippocampal (B) volumes of WT and GPR120 KO mice. Nissl staining (C-E) and pyramidal cell counts of hippocampus (C) and CA3 (E). Scale bar = 80 □m. The protein levels determined by western blot analysis (F). The protein levels of DCX in the hippocampus (G). The immunofluorescence of DCX (H) and DCX-positive cell count in the dentate gyrus (I). Scale bar = 80 □m. Ki67 staining (J) and

the number of Ki67-positive nuclei in the dentate gyrus (K). Scale bar = 80 □m. The SOD2 mRNA (L) and protein (M) expression levels in the hippocampus. The synaptophysin (Syn) (N) and PSD95 (O) protein levels in the hippocampus. Learning and memory performance were evaluated using the Y-maze (P). Data are presented as the mean ± SEM, n = 5 per group. Statistical analysis was performed using a student's t-test (*p < 0.05; **p < 0.01; ***p < 0.001 vs. WT). Morris water maze test: Escape latency (Q) and Time platform crossed (R). Data are mean ± SEM, n = 10 per group. Statistical analysis was performed using two-way ANOVA followed by post-hoc Tukey test (***p < 0.001 vs. WT).

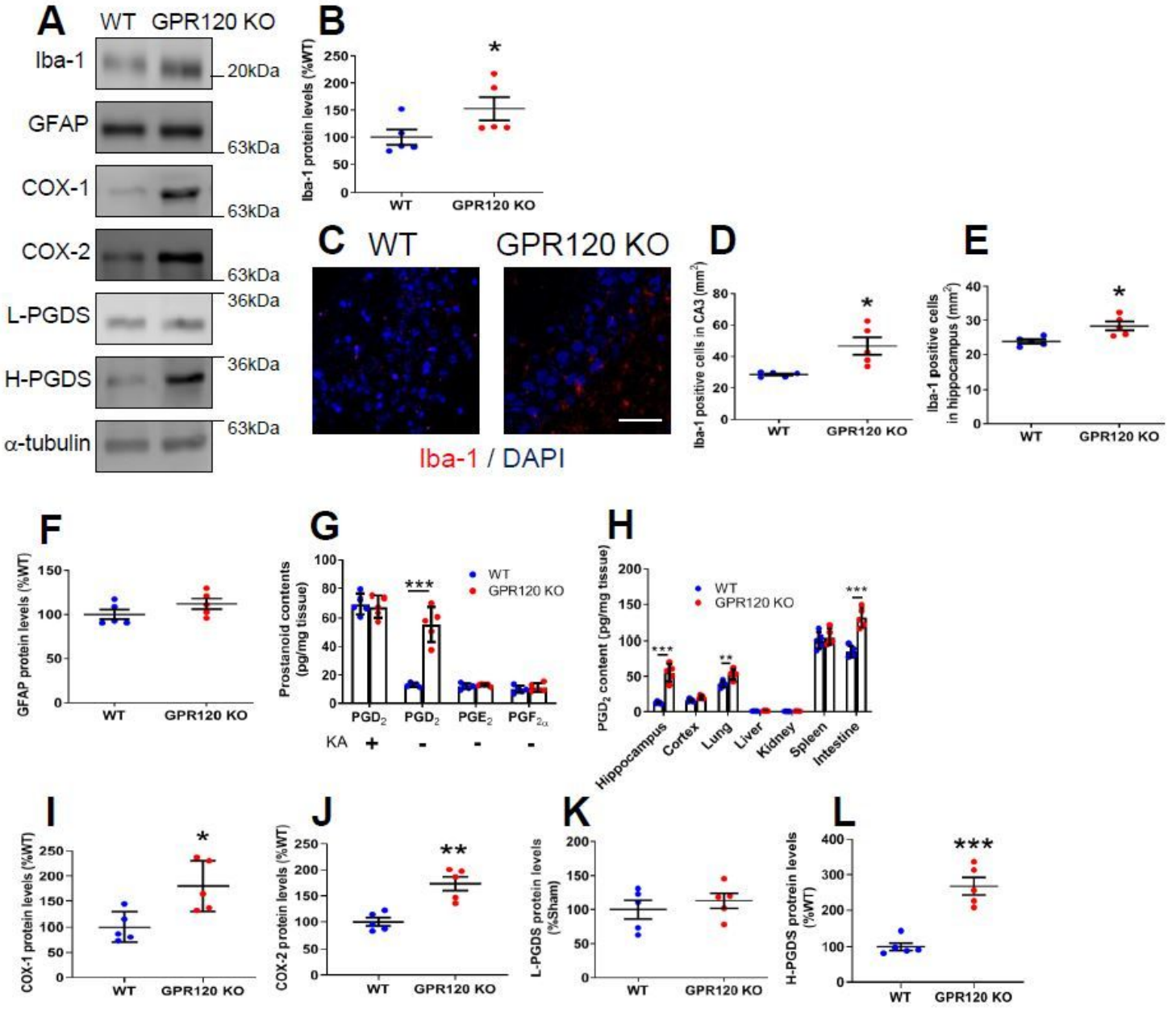

Figure 2

Microglial activation and PGD2 production observed in the hippocampus of WT and GPR120 KO mice. The protein levels determined by western blot analysis (A). The protein levels of Iba-1 in the hippocampus (B). The immunofluorescence of Iba-1 (C-E) and Iba-1 positive cell counts in the CA3 (D) and

hippocampus (E). Scale bar = 50 □m. The protein levels of GFAP in the hippocampus (F). PGD2, PGE2, and PGF2□ contents (G) in the hippocampus. PGD2 contents in each tissue (H). The protein levels of COX-1 (I), COX-2 (J), L-PGDS (K), and H-PGDS (L) in the hippocampus. Data are means ± SEM, n = 5 per group. Statistical analysis was performed using unpaired Student's t-test (*p < 0.05; **p < 0.01; ***p < 0.001 vs. WT).

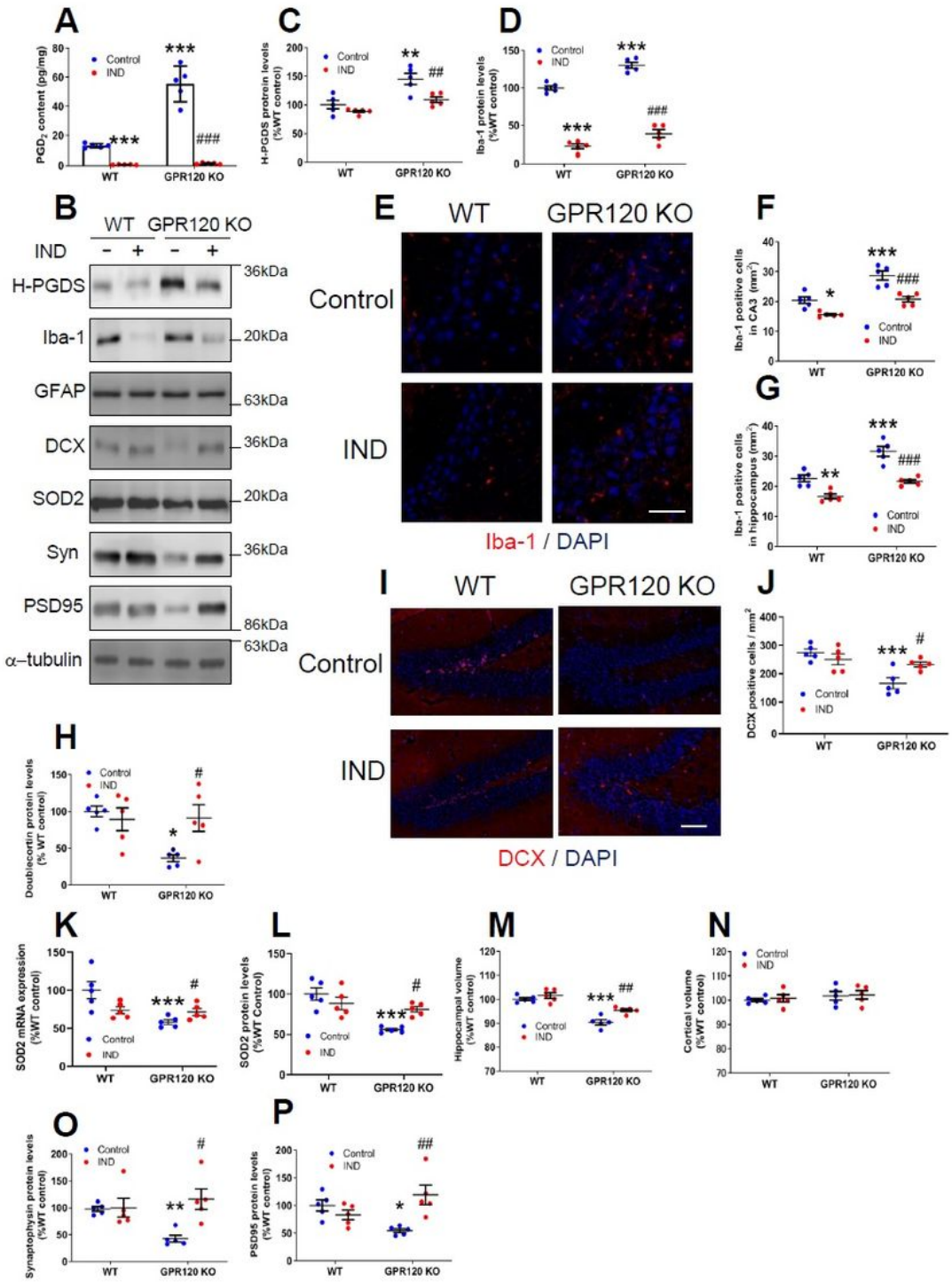

Figure 3

Inhibition of PGD2 suppressed microglial activation and prevented the neurodegeneration in the GPR120 KO mice. WT and GPR120 KO mice were administrated indomethacin (IND) for 11 weeks. PGD2 contents in the hippocampus (A). The protein levels determined by western blot analysis (B). The protein levels of H-PGDS (C) and Iba-1 (D) in the hippocampus. Immunofluorescence staining of Iba-1 (E) and Iba-1-positive cell counts in the CA3 (F) and hippocampus (G). Scale bar = 50 □m. The protein levels of DCX in the hippocampus (H). The immunofluorescence of DCX (I) and DCX-positive cell counts in the dentate gyrus (J). Scale bar = 80 □m. The SOD2 mRNA (K) and protein (L) expression levels in the hippocampus. Hippocampal (M) and cortical (N) volume of WT and GPR120 KO mice. The synaptophysin (Syn) (O) and PSD95 (P) protein levels in the hippocampus. Data are mean ± SEM, n = 5 per group. Statistical analysis was performed using two-way ANOVA followed by post-hoc Tukey test (*p < 0.05; **p < 0.01; ***p < 0.001 vs. WT control, #p < 0.05; ##p < 0.01; ###p < 0.001 vs. GPR120 KO control).

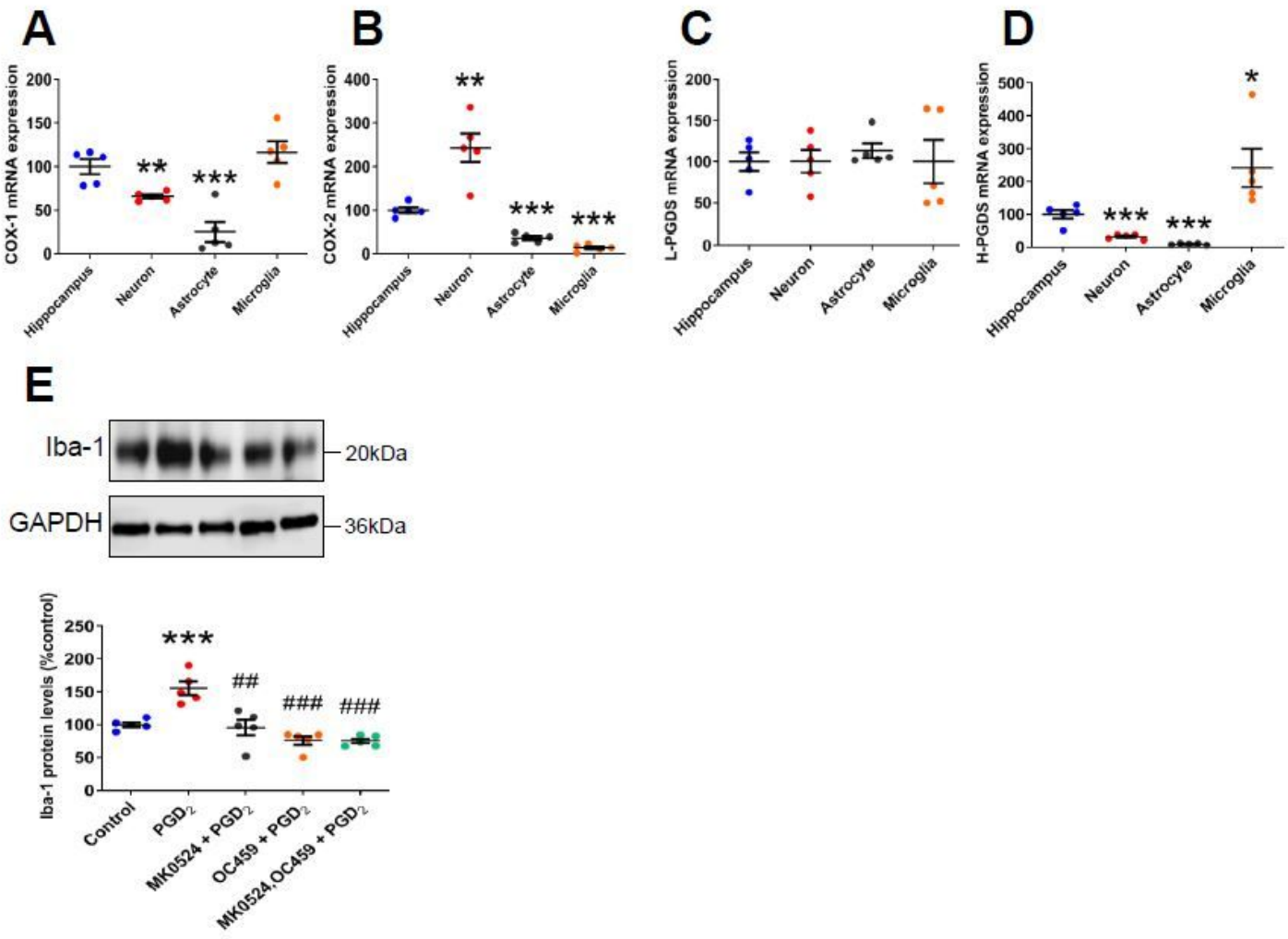

Figure 4

Expression of PGD2 synthesis enzymes and an autocrine manner of microglial activation by PGD2. Expression of COX-1 (A), COX-2 (B) L-PGDS (C), and H-PGDS (D) mRNA in the WT hippocampal tissue and primary cultures of Neurons, Astrocytes, and Microglia. Data are mean ± SEM, n = 5 per group. Statistical analysis was performed using one-way ANOVA followed by post-hoc Newman-Keuls test (*p <

0.05; **p < 0.01; ***p < 0.001 vs. Hippocampus). The protein levels of Iba-1 in the primary microglia stimulated with PGD2 1 h after addition of DP antagonists (E). Data are mean ± SEM, n = 5 per group. Statistical analysis was performed using one-way ANOVA followed by post-hoc Newman-Keuls test (***p < 0.001 vs. Control, ##p < 0.01; ### p < 0.001 vs. PGD2).

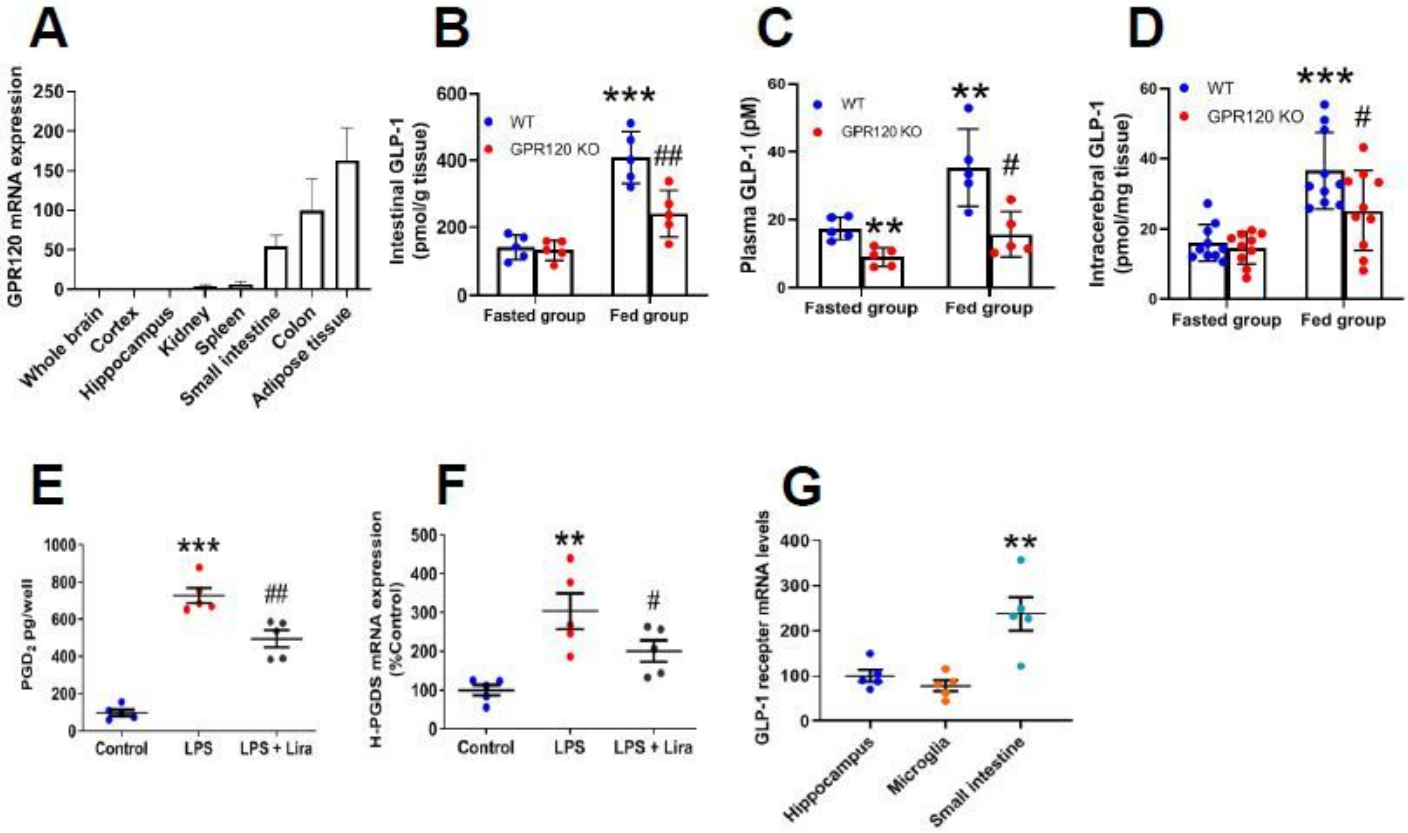

Figure 5

GPR120 mRNA expression profiles, tissue levels of GLP-1, and Liraglutide reduced microglial PGD2 production. The mRNA levels of GPR120 (A) relative to PGK1 in WT mice tissues, as determined by real-time PCR. GLP-1 contents in intestine (B), plasma (C), and whole brain (D) of WT and GPR120 KO mice. Data are presented as the mean ± SEM, n = 5 or 10 per group. Statistical analysis was performed using two-way ANOVA followed by post-hoc Tukey test (**p < 0.01; ***p < 0.001 vs. WT Fasted group, #p < 0.05; ##p < 0.01 vs. WT Fed group). PGD2 contents in the primary microglia stimulated with LPS for 1 h with liraglutide (Lira) addition (E). The mRNA expression levels of H-PGDS relative to PGK1 in primary microglia (F). Data are mean ± SEM, n = 5 per group. Statistical analysis was performed using one-way ANOVA followed by post-hoc Newman-Keuls test (**p < 0.01; ***p < 0.001 vs. Control, #p < 0.05; ##p < 0.01 vs. LPS). The mRNA expression levels of GLP-1 receptor relative to PGK1 in hippocampus, microglia, and small intestine (G). Data are mean ± SEM, n = 5 per group. Statistical analysis was performed using one-way ANOVA followed by post-hoc Newman-Keuls test (**p < 0.01 vs. Hippocampus).

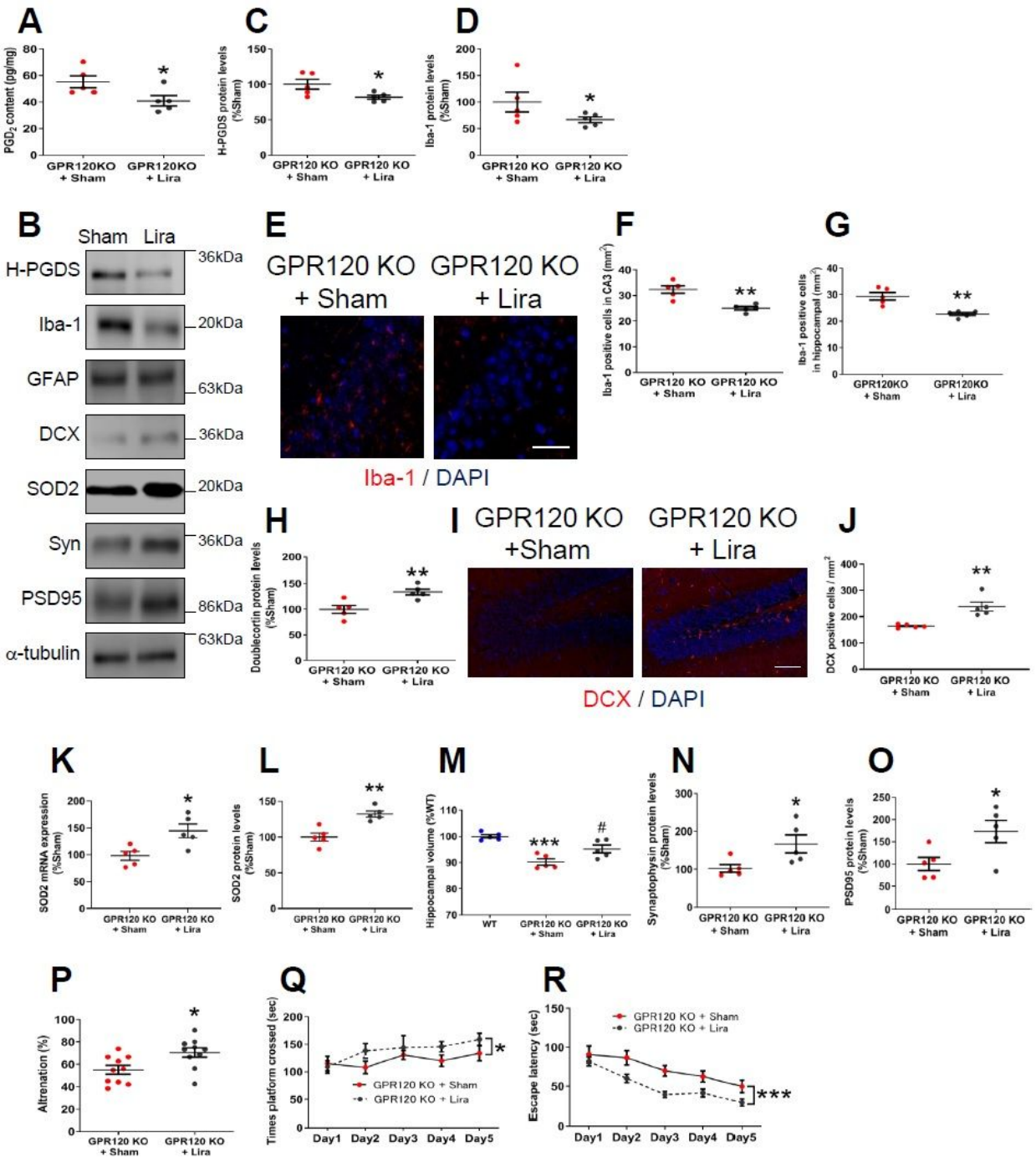

Figure 6

Liraglutide treatment reduced PGD2-microglia-provoked neuroinflammation and further neurodegeneration in GPR120 KO mice. GPR120 KO mice were administrated liraglutide (Lira) peripherally for 11 weeks. PGD2 contents in the hippocampus (A). The protein levels determined by western blot analysis (B). The protein levels of H-PGDS (C) and Iba-1 protein levels (D) in the hippocampus. The immunofluorescence of Iba-1 (E) and Iba-1-positive cell counts in the CA3 (F) and hippocampus (G). Scale bar = 50 □m. The protein levels of DCX the hippocampus (H). The

immunofluorescence of DCX (I) and DCX-positive cell counts in the dentate gyrus (J). Scale bar = 80 □m. The SOD2 mRNA (K) and protein (L) expression levels. Data are presented as the mean ± SEM, n = 5 per group. Statistical analysis was performed using a student's t-test (*p < 0.05; **p < 0.01 vs. GPR120 KO + Sham). Hippocampal volume of WT and GPR120 KO mice, and Liraglutide-treated GPR120 KO mice (M). Statistical analysis was performed using one-way ANOVA followed by Newman-Keuls post-hoc test (***p < 0.001 vs. WT, #p < 0.05 vs. GPR120 KO + Sham). The synaptophysin (Syn) (N) and PSD95 (O) protein levels in the hippocampus. Learning and memory performance were evaluated using the Y-maze (P). Data are presented as the mean ± SEM, n = 5 per group. Statistical analysis was performed using a student's t-test (*p < 0.05 vs. GPR120 KO + Sham). Morris water maze test: Escape latency (Q) and Time platform crossed (R). Data are mean ± SEM, n = 10 per group. Statistical analysis was performed using two-way ANOVA followed by post-hoc Tukey test (*p < 0.01; ***p < 0.001 vs. WT).

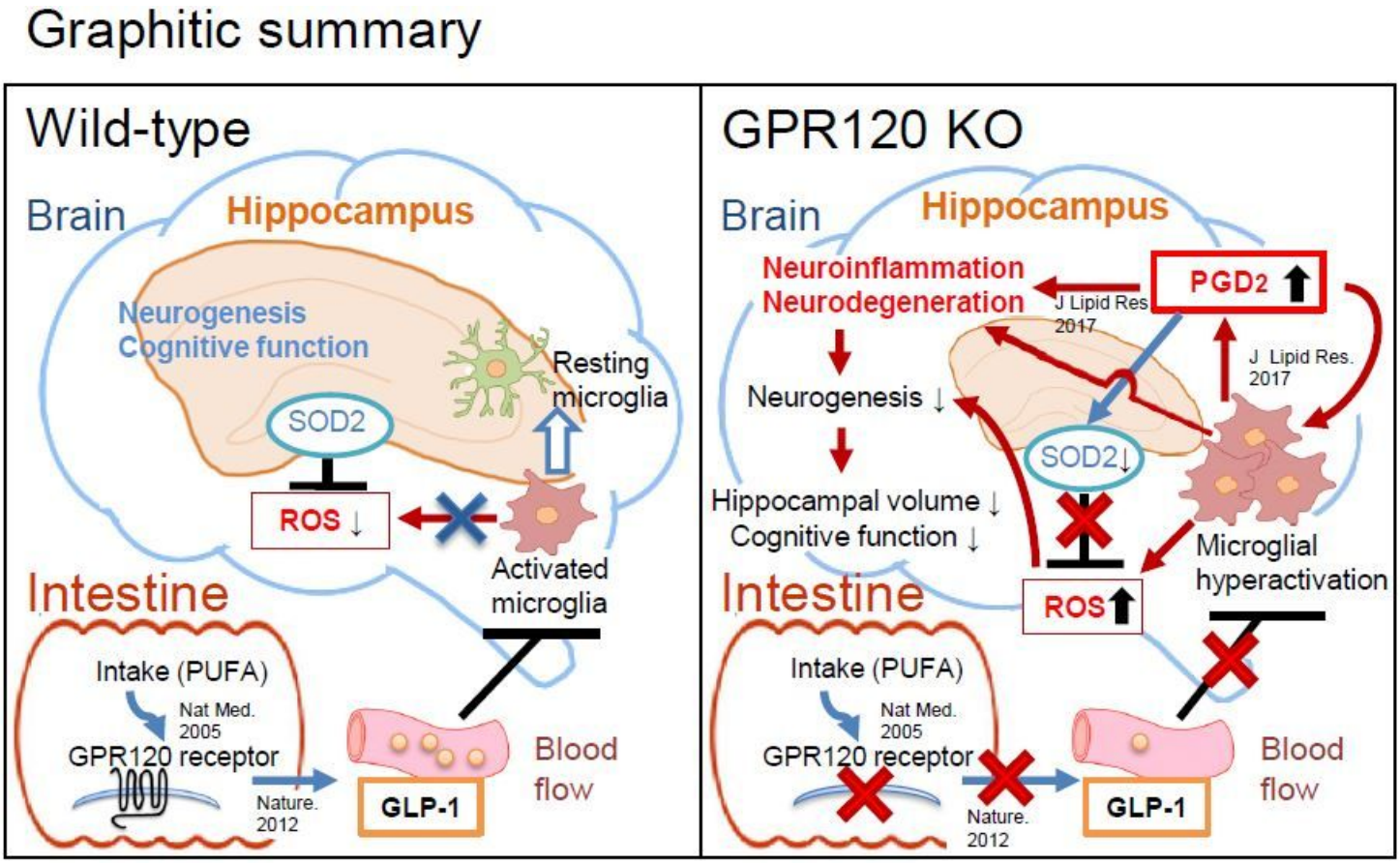

Figure 7

Dysfunction of peripheral GPR120 caused PGD2-microglia-provoked neuroinflammation and neurodegeneration in the hippocampus. Peripheral GLP-1 by intestinal GPR120 stimulation remotely contributed to hippocampal homeostasis via suppression of PGD2-microglia-provoked neuroinflammation in WT mice. However, insufficient GLP-1 bioactivity caused by GPR120 dysfunction induced PGD2-microglia-provoked neuroinflammation and neurodegeneration in GPR120 KO mice.

Supplementary Files

This is a list of supplementary files associated with this preprint. Click to download.

- Additionalfile1.pdf
- Additionalfile2.pdf
- Additionalfile3.pdf
- Additionalfile4.pdf